Final Draft
of the original manuscript:

Song, J.; Wang, Z.; Huang, Y.; Srinivasan, A.; Beckmann, F.; Kainer, K.U.; Hort, N.:

Hot tearing characteristics of Mg–2Ca–xZn alloys

In: Journal of Materials Science (2015) Springer

DOI: 10.1007/s10853-015-9583-y

Hot tearing characteristics of Mg–2Ca–xZn alloys

J. Song[1] and Z. Wang[2], Y. Huang[1], A. Srinivasan[3], F. Beckmann[1], K.U. Kainer[1], N. Hort[1]

[1]Institute of Materials Research, Helmholtz-Zentrum Geesthacht, Geesthacht, Germany
[2]School of Materials Science and Engineering, Shenyang University of Technology, Shenyang 110870, China
[3]CSIR-National Institute for Interdisciplinary Science and Technology, Pappanamcode (P.O), Thiruvananthapuram 695 019, India

Abstract

Influence of Zn content (0, 0.5, 1.5, 4 and 6 wt%) on the hot tearing characteristics of Mg–2 wt% Ca alloy was investigated. The constrained rod casting (CRC) apparatus equipped with a load cell and data acquisition system was used. The initiation of hot tearing was monitored during solidification. The effect of mould temperatures (250 and 450 °C) on the hot tearing was also investigated. The formed tears were evaluated using X-ray tomography and the tear volumes were measured. Results show that hot tearing susceptibility (HTS) of Mg–2Ca–xZn (x = 0, 0.5, 1.5, 4 and 6 wt%) alloys increases with increase in Zn content up to 1.5 wt%, then decreases with further increase in the Zn content to 6 wt%. Higher initial mould temperature (450 °C) improves the hot tearing resistance. The observations on the microstructures and the fracture surfaces suggest that the hot tear initiated at the grain boundaries and propagated along them through the thin liquid film rupture and liquid metal embrittlement of solid bridges. Tear healing by low melting point eutectic liquid is also observed in some of the alloys.

1 Introduction

Hot tearing is a common and serious defect occurring during solidification of alloys [1]. The tears can compromise a cast component's structural integrity, lead to a loss of pressure tightness and act as stress raisers aiding in the propagation of fatigue cracks or catastrophic failure. Thus, tear-free castings are highly desirable for the subsequent processing and service [2]. Hot tearing occurs above the solidus temperature, often at hot spots where the casting solidifies last or at areas with sudden changes of cross section [3]. Normally, the volume fraction of solid at the hot tearing stage is in the range of 85–95 % and the solid phase is organised in a continuous network of grains [4].

Hot tearing is complex because of many factors that can influence it [5] and is not fully understood yet. Hot tearing behaviour of several binary Mg alloys has been investigated, such as Mg–Al [6, 7], Mg–Zn [8], Mg–Y [9] and Mg–Gd [10]. In addition, hot tearing behaviour of the ternary Mg–Zn–Y [11, 12], Mg–Ca–Al [13], Mg–Sr–Al [3, 14] and Mg–Zn–Al [15, 16] alloys has also been investigated. Results revealed that hot tearing susceptibility (HTS) is composition dependent. Zhou et al. [8] reported that Mg–1.5 wt% Zn is the most susceptible to hot tearing within the range of Mg–(0.5–12) wt% Zn. Y is found to have a positive effect on hot tearing resistance of Mg–Zn–Y alloys as its addition shortens the freezing range (FR) of Mg–Zn–Y alloys [12]. Similarly, increase in Ca content (0.5–3.5 wt%) is found to decrease the HTS of Mg–4Al– xCa ternary alloys, while change in Al content (4–6 wt%) did not affect the HTS of Mg–2.5Ca–Al alloys [13]. It has been shown that hot tearing resistance is enhanced with increasing the contents of both Sr and Al in Mg–Al–Sr ternary alloys [3]. In addition, Zhen et al. [7] studied the effects of initial mould temperatures on hot tearing tendency of Mg–Al alloys and reported that the HTS decreased with increasing the mould temperature. Similar results can also be found from the investigations of Zhou et al. [8], Wang et al. [9] and Srinivasan et al. [10].

Mg–Zn–Ca ternary alloys have a great potential for biocompatible and automotive applications [17]. Zhang et al. [18, 19] carried out a series of investigations on biodegradable ternary Mg–Zn–Ca alloys. The mechanical properties can be tailored by adjusting the ratio of Zn to Ca. Moreover, both in vitro and in vivo studies showed that the designated Mg–Zn–Ca ternary alloys are biocompatible and have a satisfactory corrosion resistance. Previous investigations also showed that Mg–Zn–Ca alloys have an excellent creep resistance [20, 21]. Their mechanical properties as well as corrosion resistance can be further improved by subsequent thermomechanical processing [22], heat treatments [23, 24], further alloying [20, 25] and surface treatment [26].

As most of the Mg alloys are first prepared by casting, their ingots must have superior quality without casting defects in further processing. Hence their casta-

bility, especially the resistance to hot tearing must be an important casting characteristic to be investigated [14]. Previous investigations demonstrated that Mg–2 wt% Ca alloy has the most interesting hot tearing behaviour among all investigated binary Mg–Ca alloys and has a moderate HTS [27]. A study by Powell et al. shows that 2 wt% of Ca is the optimum level for the castability of Mg–Ca–Sr (AXJ) alloys [28]. Due to the extensive potential applications of Mg–Zn–Ca ternary alloys, it is of great importance to investigate their hot tearing behaviour. Consequently, in the present work the effect of Zn addition on hot tearing behaviour of Mg–2Ca–xZn alloys was investigated.

2 Experimental

2.1 Casting

Ternary Mg–2Ca–xZn (x = 0, 0.5, 1.5, 4, and 6 wt%) alloys were prepared using pure Mg, pure Ca and pure Zn. About 350 g Mg was melted in a mild steel crucible under a protective gas mixture of high pure Ar + 0.2 % SF_6. Pure Ca and Zn was added to molten Mg at 700 °C, and manually stirred for 2 min. Then the melt was heated to 750 °C, kept for 5 min, and cast into a constraint rod casting (CRC) mould. The mould was coated with a thin layer of boron nitride (a-BN, hexagonal), and preheated to 250 or 450 °C. Cooling rate in this study is defined as temperature change in whole solidification range divided by the corresponding solidification time. The calculated cooling rates of alloys are around 0.56 and 0.22 °C/s at T_{mould} = 250 and 450 °C, respectively. The cast was extracted from the mould after air cooling. For each alloy the hot tearing test was repeated for at least three times.

The actual chemical compositions of the castings were analysed using spark optical emission spectroscopy (OES) (Spectroflame, Spectro, Kleve, Germany), as listed in Table 1. Most of the actual compositions were close to the nominal compositions. The actual Ca content is lower than the nominal composition in the high-Zn-containing alloys.

2.2 Hot tearing setup

The detailed description on the hot tearing setup can be found elsewhere [9]. Briefly, the setup consists of a CRC mould, a temperature monitor and measurement unit, a contraction force measurement unit with a load cell (connected to the load screw). The schematic CRC mould used in this study is shown in Fig. 1a. Due to the temperature difference, the casting at the rear end solidified at first and the surrounding Mg casting enwrapped the load screw. As the load screw was

	Ca	Zn	Fe	Mn	Si	Mg
Mg2-Ca	1.91	-	0.00411	0.0393	0.0107	Bal.
Mg-2Ca-0.5Zn	1.98	0.51	0.00437	0.0394	0.0123	Bal.
Mg-2Ca-1.5Zn	0.194	1.49	0.00449	0.0381	0.0133	Bal.
Mg-2Ca-4Zn	1.72	4.07	0.00665	0.0420	0.0160	Bal.
Mg-2Ca-4Zn	1.64	6.49	0.00548	0.0371	0.0143	Bal.

Table 1: Actual chemical compositions of the cast Mg–2Ca–xZn alloys (wt%)

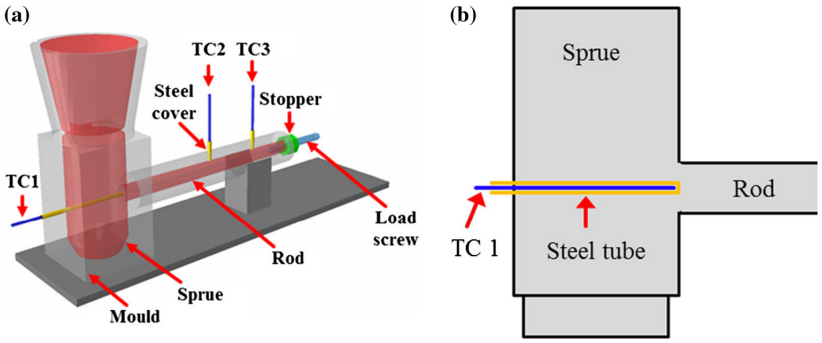

Figure 1: Schematic of a the CRC mould; b the location of the thermocouple. TC - thermocouple

fixed, a constraint was generated in the axial direction of the casting rod. Consequently, a hot tear might occur at the hot spot as a result of such constraint. Besides, the present CRC mould differed from Cao et al.'s mould [6] as the rod portion of the mould was designed with a taper (diameter decreased from 12.5 mm at the junction to 10 mm at the end of the rod), as shown in Fig. 1a. This unique design successfully eliminated the influence of friction between the mould and casting rod, which ensured the collected contraction force data more reliable.

During solidification, the temperature at hot spot (TC 1) and the force were simultaneously recorded. The thermocouple 1 located at the exact sprue-rod junction (hot spot), as shown in Fig. 1b. All the thermocouples were inserted in steel tubes and firmly fixed on the mould. The principle of the apparatus is to monitor the evolution of hot tearing using the measurement of the contraction force and temperature. Generally, the hot tearing initiation and propagation was determined through the force release. Thus, a force drop was normally considered as the initiation of the hot tearing. Besides, by analysing the force evolution during solidification, the final size of the hot tear can also be investigated. With the simultaneously recorded temperature, the corresponding solid fraction of hot

tearing initiation was determined with Pandat software. As a result, the relation between solidification path and hot tearing is established.

2.3 Characterisation of microstructures, fracture surfaces and second phase

The microstructures and tear morphologies were investigated by optical microscope (OM, LEICA DMI5000 M microscope, Germany) and scanning electron microscope (SEM, Zeiss Ultra 55 SEM, Germany). The SEM is equipped with Energy Dispersive X-ray Spectroscopy (EDS). The samples for microstructural observations were cold mounted, ground with SiC abrasive paper (grits size from 120, 500, 800, 1200 to 2500) and polished with water free OPS and 1 lm diamond suspension. The polished samples were chemically etched in a solution with 8 g picric acid, 5 ml acetic acid, 10 ml distilled water and 100 ml ethanol. The fracture surfaces of castings with a severe tear were observed by SEM. X-ray diffraction (XRD) was carried out with a diffractometer (Siemens D5000, Germany) equipped with Cu Kα radiation to identify the constituent phases at the hot tearing area. The XRD measurement was performed at 40 kV and tube current of 40 mA over the 2Θ ranging from 10° to 90°, using a step size of 0.01° with a counting time of 5 s at each step.

2.4 X-ray tomography

Initially, the hot tears of the castings were photographed using a digital camera and visually inspected. The macroview of the hot tearing provides an intuitive and initial impression on the severity of hot tearing. X-ray microtomography was introduced to observe the tear more in detail. Using this technique, 3D images of the tear can be obtained. Also, the whole crack volume, including both the closed and open cracks, can be accurately quantified. The quantified crack volumes were used to evaluate the HTS of alloys.

The measurements were carried out in a 3D X-ray tubebased high-resolution tomography (nanotom® s– phoenix, Germany). The 3D volume reconstruction was made from the 2D projections (with a filtered back projection algorithm) using datos| 92.0 reconstruction software (phoenix, Germany). The resolution achieved after reconstruction of the volume in the interesting region was of about 20 μm.

Further data processing, including normalisation and alignment of the 3D-data sets, the segmentation and characterisation of the tear volume was applied using the software IDL 8.1. The samples consist of an original rod and a cubic from the sprue which were cut from the castings. Detailed information about samples can

be found elsewhere [29]. The crack volume of samples was calculated based on the 3D volume reconstruction results. The average crack volume of minimum two samples for each alloy was reported.

3 Results

3.1 Microstructures

Microstructures near the main tear region in Mg–2Ca–xZn alloys cast at T_{mould} = 250 °C are shown in Fig. 2a, c, e, g. Microstructure of Mg–2Ca alloy is not shown here and can e found elsewhere [27]. Eutectic (primary and Mg_2Ca) segregation is found near the main tear in Mg–2Ca alloy.

Large eutectic segregation is also evident in all four ternary Mg–Ca–Zn alloys. The detailed microstructure of the eutectic in ternary Mg–2Ca–xZn alloys is shown in Fig. 2b, d, f, h. According to the EDX results (Fig. 3), Mg_2Ca is the main second phase in Mg–2Ca–0.5Zn alloy. As the Zn content increases to 1.5 and 4 wt%, in addition to Mg_2Ca, ternary Mg6Ca2Zn3 phase is also observed. However, only the Mg6Ca2Zn3 phase is present as the second phase in Mg–2Ca–6Zn alloy. The solutes are highly segregated at the tearing area due to the nonequilibrium solidification that occurred.

Figure 4 shows the XRD patterns of alloys cast at T_{mould} = 250 °C. The second phases were identified according to the standard PDF cards. The XRD results confirm that both Mg–2Ca–0.5Zn and Mg–2Ca–1.5Zn alloys contain primary Mg and Mg_2Ca phase. However, peaks for both Mg_2Ca and $Mg_6Ca_2Zn_3$ phases are detected in Mg–2Ca–4Zn alloy. The XRD pattern of Mg–2Ca–6Zn alloy consists of peaks for primary Mg and ternary Mg6-Ca2Zn3 phase. Although SEM observations indicated the presence of the ternary $Mg_6Ca_2Zn_3$ phase in Mg–2Ca–1.5Zn alloy, it is not detected by XRD, suggesting that the amount of $Mg_6Ca_2Zn_3$ in this alloy is below the detection limit of XRD.

The microstructures near the tear region in Mg–2Ca–xZn alloys cast at a higher initial mould temperature (T_{mould} = 450 °C) are displayed in Fig. 5a, c, e, g. Similar as displayed in Fig. 2, the second phases are identified and marked in Fig. 5b, d, f, h. These microstructures are different from those of the alloys cast at T_{mould} = 250 °Cin several ways. Firstly, the volume of eutectic or second phase at the hot spot is much less than that observed at the lower mould temperature. This indicates that the solute segregation at the high mould temperature, 450 °C, is lower than that at the low mould temperature, 250 °C, which is likely due to the homogenous distribution of solute at a low cooling rate (high initial mould temperature). Secondly, more Mg_2Ca particles are found in the Mg–2Ca–0.5Zn,

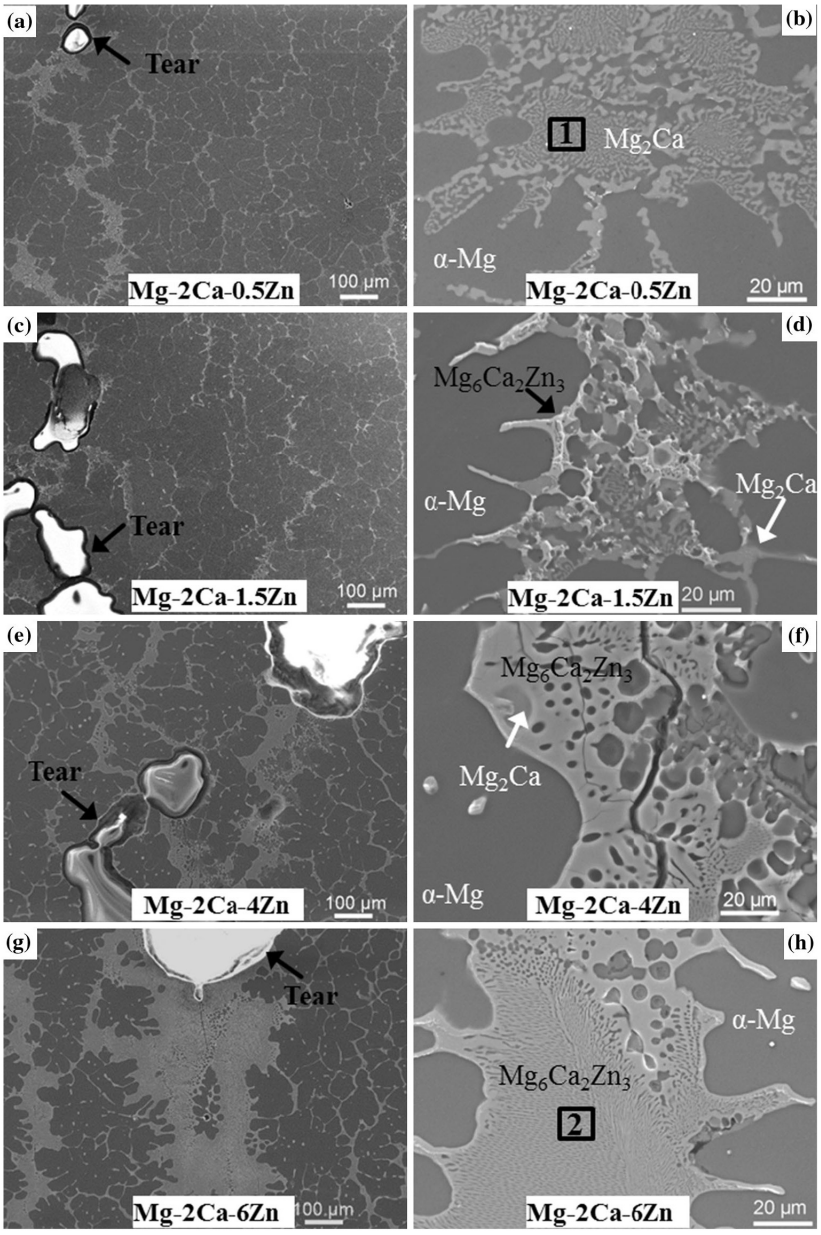

Figure 2: Microstructures at hot spots of Mg–2Ca–xZn alloys cast at T_{mould} = 250 °C, a, b Mg–2Ca–0.5Zn; c, d Mg–2Ca–1.5Zn; e, f Mg–2Ca– 4Zn; and g, h Mg–2Ca–6Zn

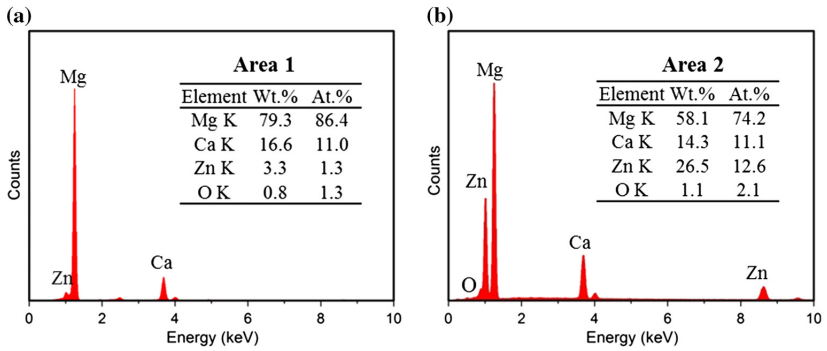

Figure 3: EDS analysis of Mg–2Ca–xZn alloys, a area 1 (Mg_2Ca) in Fig. 2b; b area 2 ($Mg_6Ca_2Zn_3$) in Fig. 2h

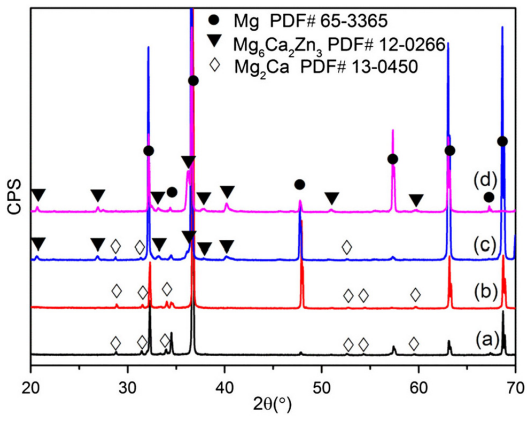

Figure 4: XRD patterns of alloys cast at T_{mould} = 250 °C, a Mg–2Ca– 0.5Zn; b Mg–2Ca–1.5Zn; c Mg–2Ca–4Zn; and d Mg–2Ca–6Zn

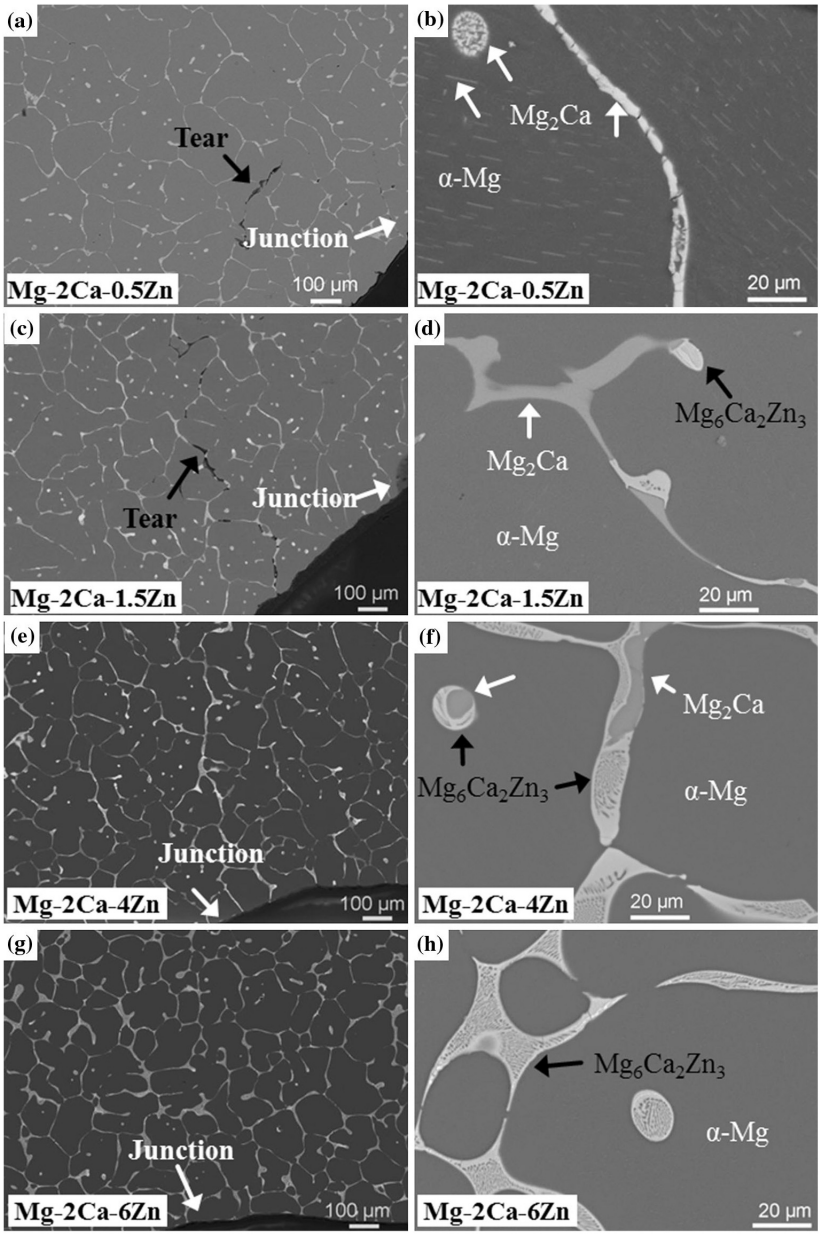

Figure 5: Microstructures at hot spots of Mg–2Ca–xZn alloys cast at T_{mould} = 450 °C, a, b Mg–2Ca–0.5Zn; c, d Mg–2Ca–1.5Zn; e, f Mg–2Ca– 4Zn and g, h Mg–2Ca–6Zn

Mg–2Ca–1.5Zn and Mg–2Ca–4Zn alloys. Finally, more $Mg_6Ca_2Zn_3$ is observed in the Mg–2Ca– 1.5Zn alloy.

3.2 Force–temperature–time curves

The as-recorded force–temperature–time curves of Mg– 2Ca–xZn alloys cast at a mould temperature of 250 °C are displayed in Fig. 6. As Mg–2Ca alloy has a high solidus temperature of 517 °C, the force–temperature–time curve was recorded only for 692 s. By comparing the overall force–temperature–time curves (Fig. 6a–e), it is observed that Mg–2Ca–0.5Zn alloy displays a rough plateau after the termination of crack propagation. This observation indicates that the Mg–2Ca–0.5Zn sample was completely broken (severe HTS). Moreover, multiple force drops in the force curve of Mg–2Ca and Mg–2Ca–6Zn alloy are noticed (Fig. 6a, e). The information about the hot tearing initiation and termination is provided by these curves [9], as marked on the figures. The typical determination of hot tearing initiation is shown in detail in Fig. 6f. Normally, a force drop (Fig. 6a) or a sudden force slope change (Fig. 6f) is regarded as the initiation of hot tearing. Both of them reveal the stress relaxation caused by the formation of hot tears [30, 31]. In addition, the solid fraction (mole fraction) at hot tearing initiation, f_{si} is found low for all the Mg–2Ca–xZn alloys. The fsi values of Mg–2Ca, Mg–2Ca–0.5Zn, Mg–2Ca–1.5Zn, Mg–2Ca–4Zn and Mg–2Ca–6Zn alloys are 0.890, 0.648, 0.759, 0.519 and 0.814, respectively. All the f_{si} values are lower than 0.9.

Figure 7 shows the force–temperature–time curves of Mg–2Ca–xZn alloys cast at the mould temperature of 450 °C. Similar to the curves shown in Fig. 6a, the curve of Mg–2Ca is recorded only for 1892 s. No force drops are observed on the curves for all alloys, indicating that no tear occurred in these alloys. Interestingly, the increase in force for Mg–2Ca–6Zn alloy is slower than that for other four alloys, which is attributed to its larger freezing range (FR).

According to the thermodynamic calculations using the Pandat software, the FR of Mg–2Ca–(0.5–4) Zn alloys is from 244 to 234 °C, whereas the FR of Mg–2Ca–6Zn is 327 °C. According to the software, the solidification ends with a binary MgZn phase in Mg–2Ca–6Zn alloy which results in a solidus temperature (Ts) as low as 295 °C. On the other hand, the Ts of the other ternary alloys are 394 °C as in these cases the solidification ends with ternary $Mg_6Ca_2Zn_3$ phase. Hence, Mg–2Ca–6Zn alloy has longer solidification time. As a result, the force increment seems slow at the early stage of solidification for Mg–2Ca–6Zn alloy.

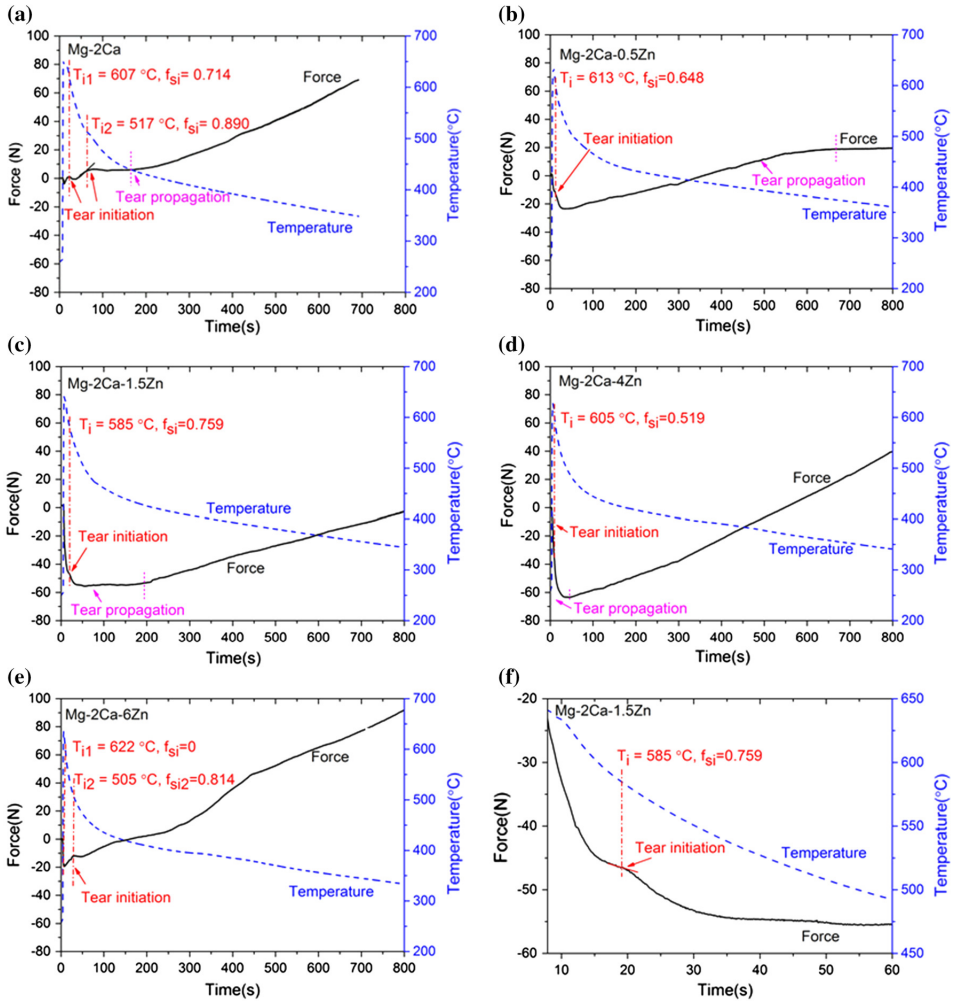

Figure 6: Overall force–temperature–time curves of alloys cast at T_{mould} = 250 °C, a Mg–2Ca; b Mg–2Ca–0.5Zn; c Mg–2Ca–1.5Zn; d Mg–2Ca–4Zn; e Mg–2Ca–6Zn and f typical determination of hot tearing initiation in Mg–2Ca–1.5Zn

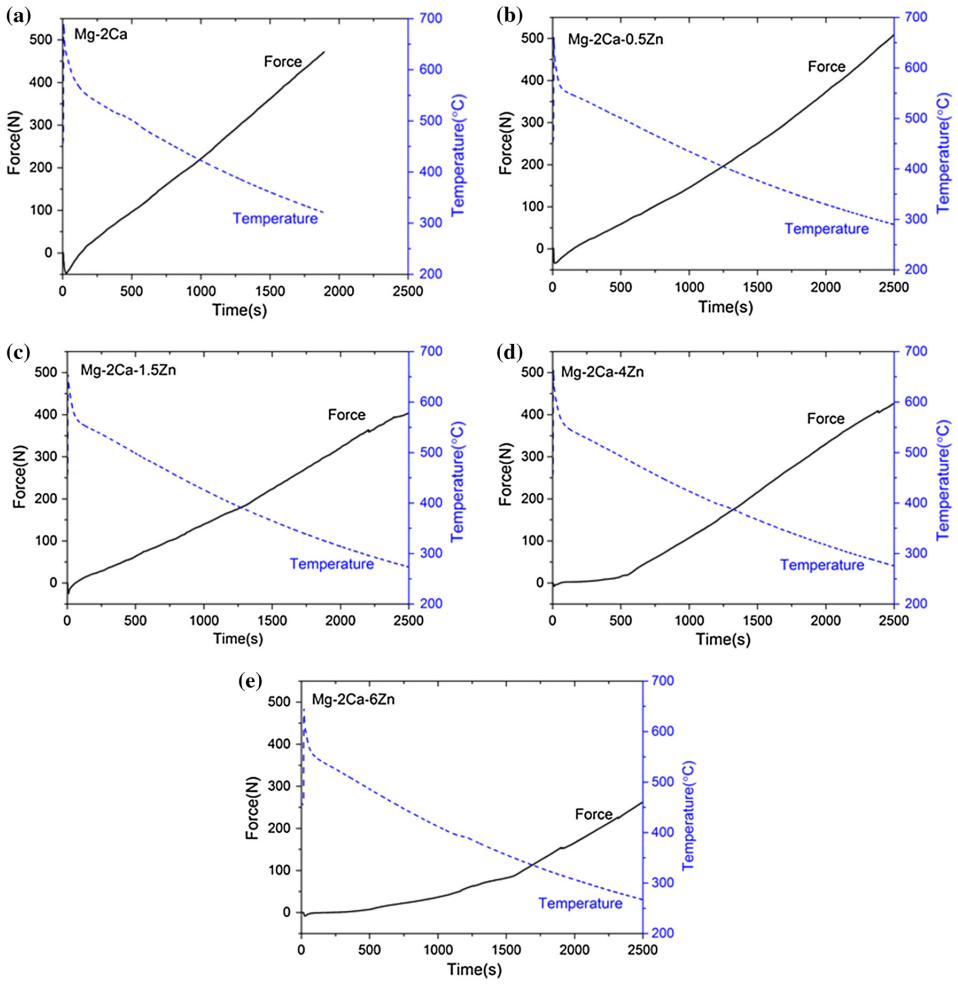

Figure 7: Force–temperature–time curves of alloys cast at T_{mould} = 450 °C, a Mg–2Ca; b Mg–2Ca–0.5Zn; c Mg–2Ca–1.5Zn; d Mg–2Ca–4Zn and e Mg–2Ca–6Zn

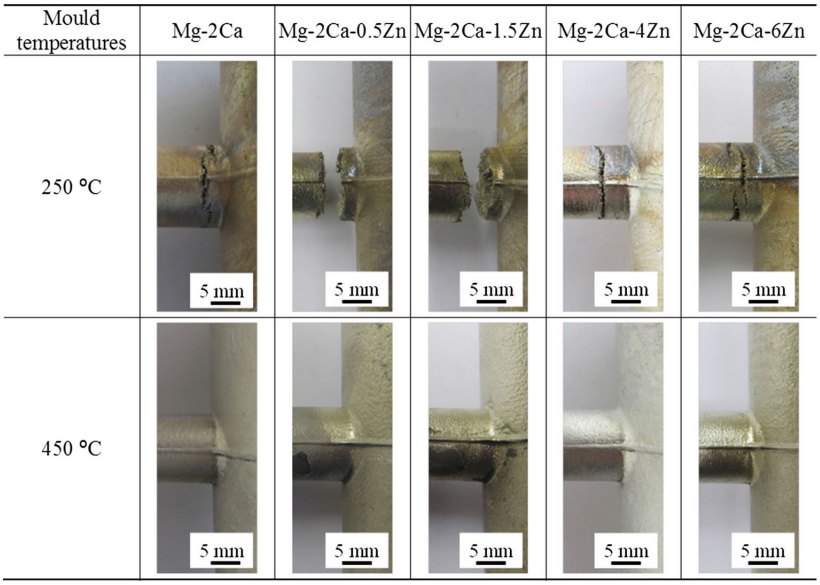

Figure 8: Macropictures of the hot tears of Mg–2Ca–xZn alloys cast at T_{mould} = 250 °C and T_{mould} = 450 °C

3.3 Hot tear evaluations

3.3.1 Macrotear morphologies

Macrophotographs of hot tears in Mg–2Ca–xZn alloy samples cast at both mould temperatures are shown Fig. 8. The in?uence of Zn content on the hot tearing of Mg–Ca–Zn alloys can be seen clearly at the mould temperature of 250 °C. As the Zn content increases the HTS of Mg–Ca–Zn alloy increases up to 1.5 wt% Zn and then decreases. The peak severity occurs at 0.5 to 1.5 wt% Zn content as the rod portion of the Mg–2Ca–0.5Zn and Mg–2Ca–1.5Zn alloys castings is completely detached from the sprue portion. Mg–2Ca and Mg–2Ca–6Zn alloys exhibit multiple cracking, which agrees well with the multiple force drops in the force–temperature–time curves (Fig. 6a, e). In addition, the tear location has moved away from the sprue-rod junction at a high Zn content. This observation may explain why all the predicted fsi using the force–temperature–time curves are lower than 0.9.

The recorded temperature was from the centre of spruerod junction area (Fig. 1b), and hence the calculated f_{si} is the solid fraction at the sprue-rod junction, not at the exact location of tearing. As the tear occurred away from the junction, the actual tear initiation temperature must be slightly lower than the measured value and hence the corresponding solid fraction must be higher. No visible tears are

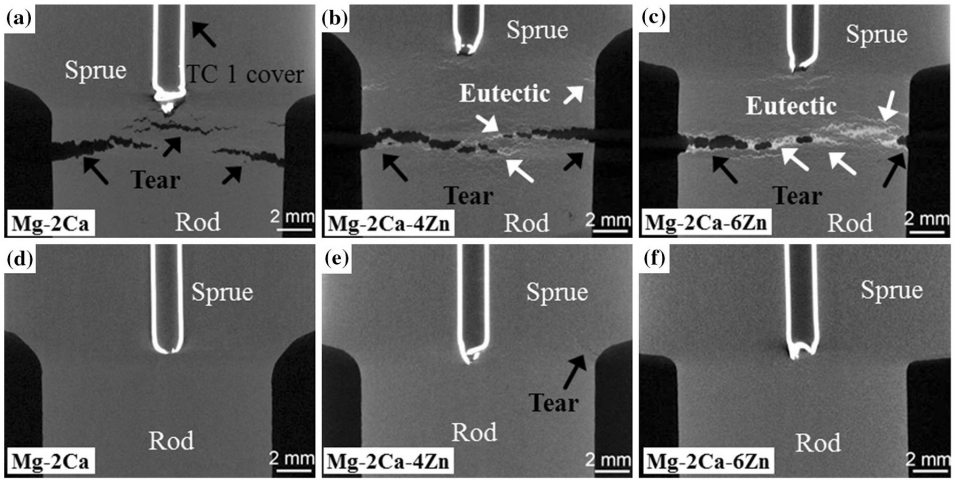

Figure 9: Longitudinal cross section (mid plane section) views of hot tears by X-ray tomography in the alloys cast at T_{mould} = 250 °C: a Mg–2Ca; b Mg–2Ca–4Zn; c Mg–2Ca–6Zn and alloys cast at T_{mould} = 450 °C: d Mg–2Ca; e Mg–2Ca–4Zn and f Mg–2Ca–6Zn

observed for all the alloys when the mould temperature increased to 450 °C, indicating that increasing the initial mould temperature is an effective way to enhance the resistance to hot tearing.

3.3.2 X-ray tomography

Longitudinal cross section (mid plane section) views of hot tears by X-ray tomography in Mg–2Ca, Mg–2Ca–4Zn and Mg–2Ca–6Zn alloys cast at both mould temperatures are shown in Fig. 9. There are few white areas (marked with white arrows) near the tear locations in Mg–2Ca–4Zn and Mg–2Ca–6Zn alloys at Tmould = 250 °C. These white areas are eutectic, as verified with EDX (Fig. 3) and XRD (Fig. 4). It is worth mentioning that eutectic is also evident in Mg–2Ca alloy. However, due to the low resolution of X-ray tomography and the similar effective atomic number of Mg2Ca (14.7) and primary Mg (12), the eutectic in Mg–2Ca is not clearly revealed.

Due to the high effective atomic number (18.4), the ternary intermetallic, $Mg_6Ca_2Zn_3$, in Mg–2Ca–4Zn and Mg–2Ca–6Zn alloys, appears clearly. Besides, the eutectic mainly distributed near the tear region but not at the exact sprue-rod junction. Only a fine tear is evident at the sprue-rod junction in Mg–2Ca– 4Zn alloy at T_{mould} = 450 °C. Interestingly, the microstructures are homogeneous in all the alloys cast at the high mould temperature 450 °C, as no eutectic segrega-

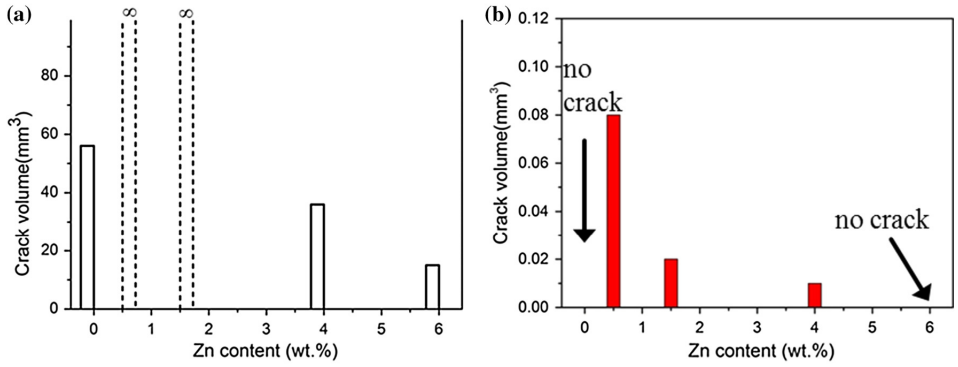

Figure 10: Crack volumes of Mg–2Ca–xZn alloys cast at different mould temperatures, a T_{mould} = 250 °C and b T_{mould} = 450 °C

tion is observed around the sprue-rod junction area. This agrees well with the homogeneous SEM micrographs shown in Fig. 5.

The measured crack volumes are shown in Fig. 10.As Mg–2Ca–0.5Zn and Mg–2Ca–1.5Zn alloys samples were completely broken, the tear volumes are displayed as dashed column in Fig. 10a. It is clear that with the increment in Zn content, the HTS of Mg–2Ca–xZn alloys firstly increases up to 1.5 wt% Zn and then decreases with further Zn addition. In general, the crack volumes of alloys cast at T_{mould} = 450 °C are relatively low (lower than 0.10 mm3). These results demonstrate again that casting at a higher mould temperature largely improves the hot tearing resistance of Mg–2Ca–xZn alloys. The measured crack volume for Mg–2Ca–6Zn alloy is zero at T_{mould} = 450 °C, indicating that no crack is observed by X-ray tomography.

3.3.3 Microtear morphologies

Polarised optical tear morphologies at the hot spot of Mg– 2Ca–xZn alloys cast at the mould temperature of 250 °C are shown in Fig. 11. All the cracks propagate along the grain boundaries. In addition, the grain sizes at the hot spot of Mg–2Ca–xZn alloys exhibit no big difference. All the five alloys show a dendritic structure at T_{mould} = 250 °C.

Figure 12 displays the tear morphologies of Mg–2Ca–xZn alloys cast at T_{mould} = 450 °C. Fine cracks are evident in the Mg–2Ca–0.5Zn and Mg–2Ca–1.5Zn alloys (as indicated by white arrow). The tears are discontinuous and located at the grain boundaries. In comparison with the microstructures of alloys at a mould temperature of 250 °C, the structures are less dendritic in nature at higher mould temperature (450 °C). This is because at a higher mould temperature, the solute has enough time to diffuse and hence well distributed.

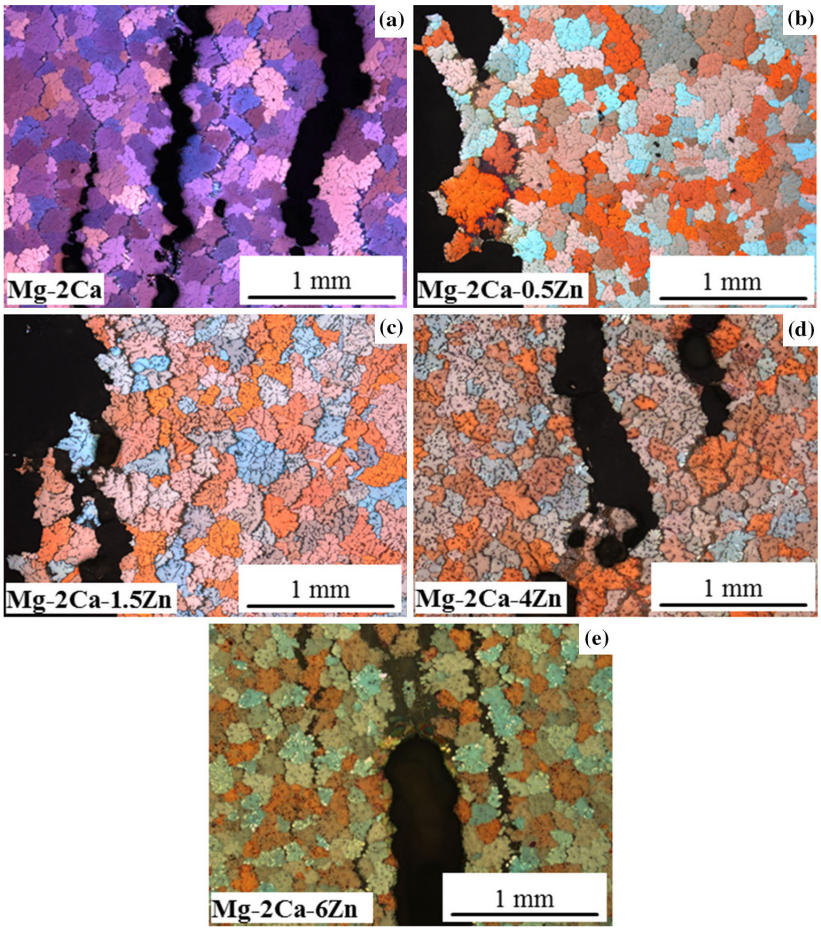

Figure 11: Optical microstructures showing tears in the alloys cast at T_{mould} = 250 °C, a Mg–2Ca; b Mg–2Ca–0.5Zn; c Mg–2Ca–1.5Zn; d Mg– 2Ca–4Zn and e Mg–2Ca–6Zn

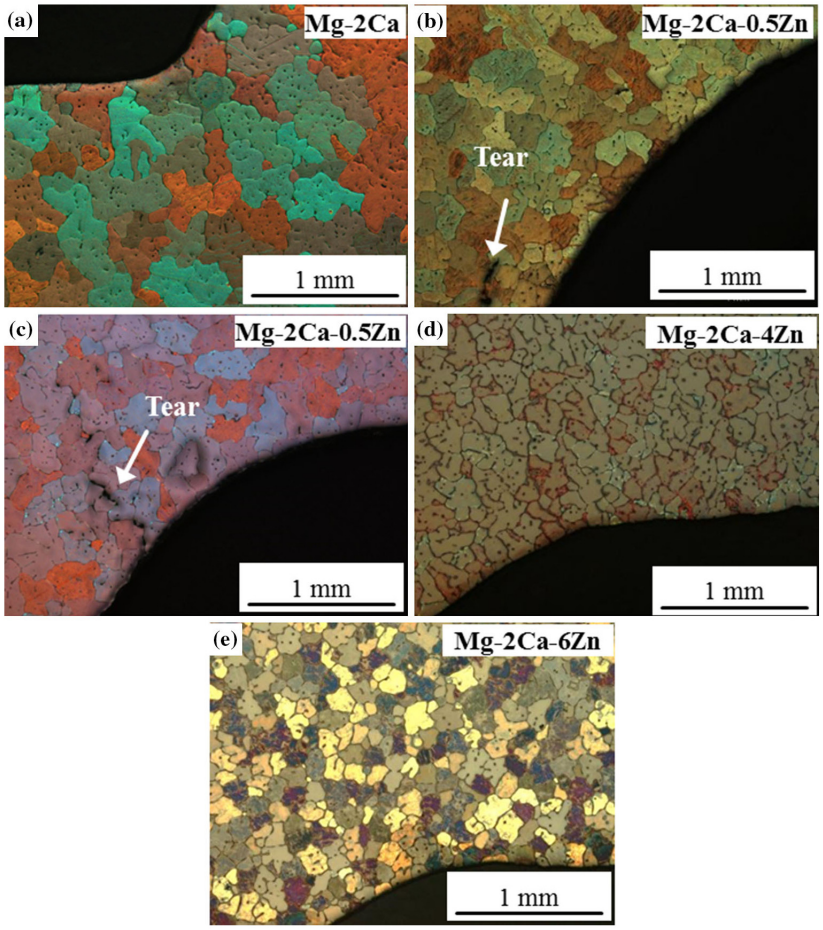

Figure 12: Optical microstructures showing tears in the alloys cast at T_{mould} = 450 °C, a Mg–2Ca; b Mg–2Ca–0.5Zn; c Mg–2Ca–1.5Zn; d Mg– 2Ca–4Zn and e Mg–2Ca–6Zn

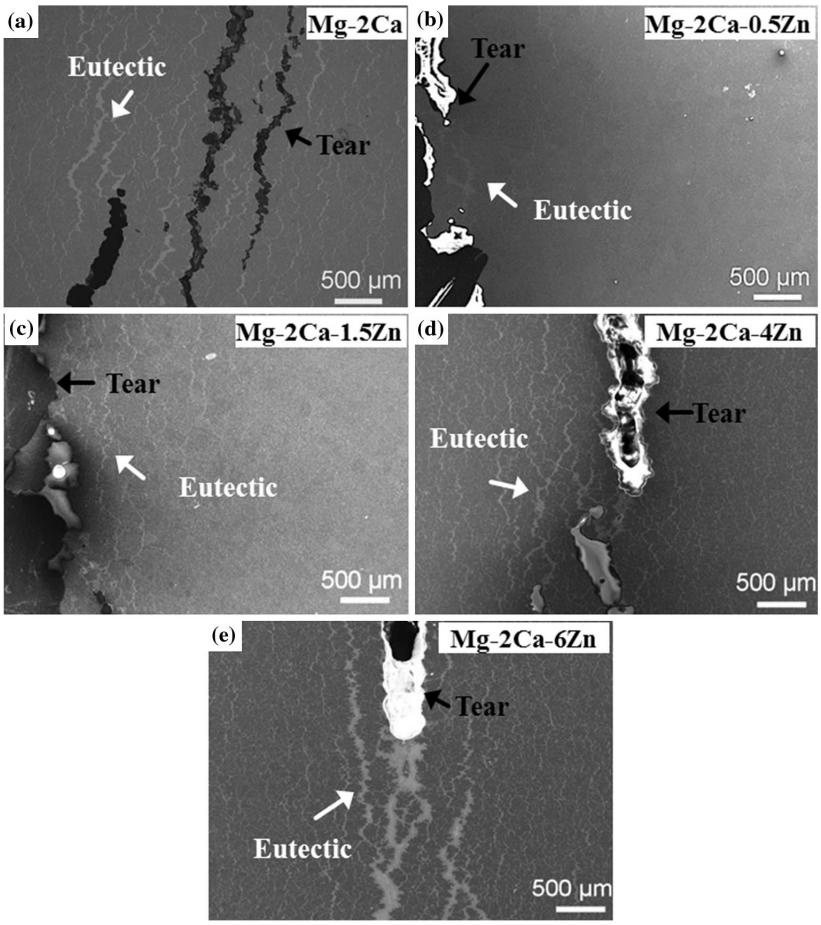

Figure 13: Eutectic distribution near the tearing region in Mg–2Ca–xZn alloys cast at T_{mould} = 250 °C, a Mg–2Ca; b Mg–2Ca–0.5Zn; c Mg–2Ca– 1.5Zn; d Mg–2Ca–4Zn and e Mg–2Ca–6Zn

3.3.4 Eutectic distribution

As previously mentioned, eutectic structure is evident in Mg–2Ca–xZn alloys cast at T_{mould} = 250 °C. In order to further analyse its distribution, SEM was carried out near tear region and the resulting micrographs are shown in Fig. 13. As the microstructures of Mg–2Ca–xZn alloys cast at T_{mould} = 450 °C are homogenous (Fig. 5), only the microstructures of the alloys cast at T_{mould} = 250 °C are shown here. As proved previously, the river-like structure with a slightly brighter colour than the matrix is confirmed as eutectic. Eutectic segregation is mainly found near the tears and its amount firstly decreases and then increases with increase in Zn content. Both Mg–2Ca and Mg–2Ca–xZn have large amount of eutectic. The

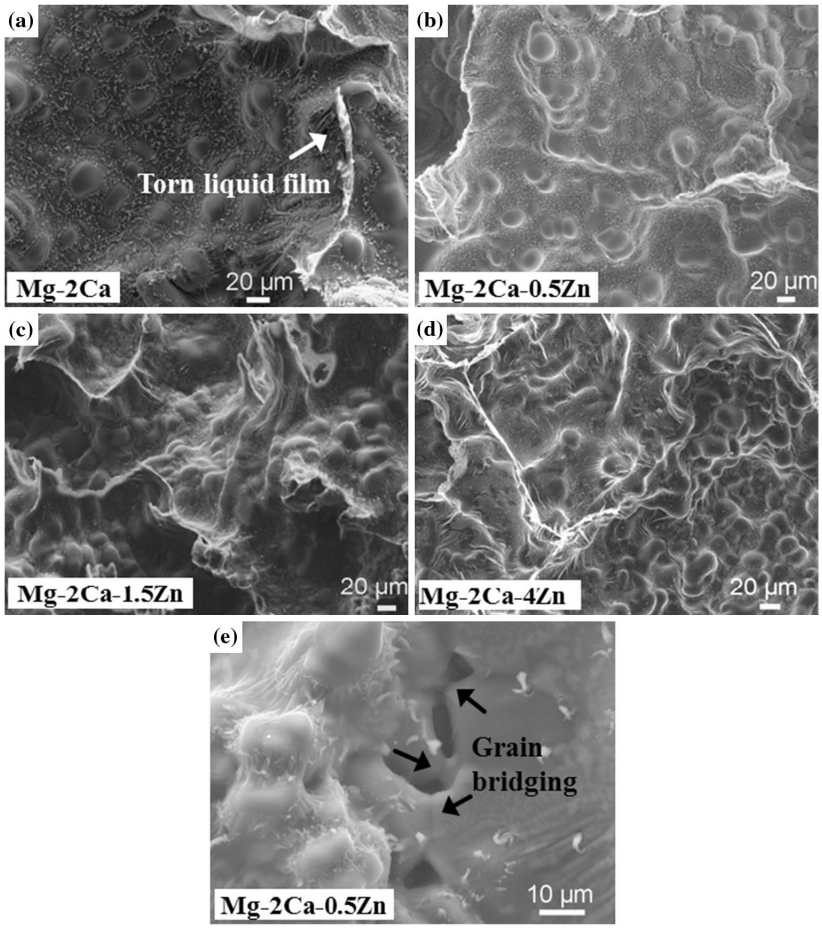

Figure 14: Fracture surfaces of alloys cast at T_{mould} = 250 °C, a Mg–2Ca, b Mg–2Ca–0.5Zn, c Mg–2Ca–1.5Zn, d Mg–2Ca–4Zn and e Mg–2Ca– 0.5Zn showing grain bridging

width of eutectic in front of the main crack tip is almost the same as the width of the tear, which is likely due to the refilling of eutectic liquid.

3.3.5 Fracture surfaces

The observations on fracture surfaces also help to understand the hot tearing behaviour of Mg alloys. Typical hot tearing fracture surfaces are observed in Mg–2Ca, Mg– 2Ca–(0.5–4) Zn alloys, as shown in Fig. 14 a–d. Evidence of ruptured liquid films is seen in all the shown fracture surfaces, which clearly proves the fact that the liquid is present during tearing. Besides, dendrites are visible in all the fracture surfaces of Mg–2Ca–xZn alloys. Inner cracks with the grain

	T_l	T_s	FR	$T_{0.9}$	$T_{0.99}$	ΔT_s
Mg2-Ca	639	517	122	517	517	0
Mg-2Ca-0.5Zn	638	394	244	507	404	103
Mg-2Ca-1.5Zn	635	394	241	486	394	92
Mg-2Ca-4Zn	628	394	234	424	394	30
Mg-2Ca-4Zn	622	295	327	394	344	50

Table 2: Calculated temperatures (°C) at different solid fractions with Scheil model for Mg–2Ca–xZn alloys, T_l: liquidus temperature, T_s: solidus temperature, FR: freezing range, $T_{0.9}$: temperature at f_s = 0.9, $T_{0.99}$: temperature at f_s = 0.99 and ΔT_s: $T_{0.9}$ - $T_{0.99}$

bridging and gaps between grains on the fracture surface of Mg–2Ca–0.5Zn alloy shown in Fig. 14e indicate that crack propagated also through liquid metal embrittlement of solid bridges. These gaps can either grow to a continuous tear or be filled by eutectic. If the contraction force exceeds the strength built up from the solid bridging, it is easy for the formed gap (crack) to propagate through the neighbouring grain bridge (liquid metal embrittlement of solid bridges [32]). If the strength built up through grain bridging is high enough to resist the crack propagation, no continuous tear will form. On the other hand, these early formed gap might be filled with eutectic, which depends on the amount of available eutectic and feeding conditions. Therefore, based on the observations of fracture surfaces, it is concluded that the possible tearing propagation mechanism is liquid film rupture as well as liquid metal embrittlement of solid bridges.

4 Discussion

4.1 Effect of Zn addition

The present study indicates that the HTS of Mg–2Ca–xZn alloys firstly increases with increase in Zn content up to 1.5 wt%, and then decreases with further Zn addition. Previous studies show that the HTS of Mg–2Ca–xZn alloys are in?uenced by Zn content in the following ways: susceptible freezing range (ΔT_s, temperature range of a solid fraction (f_s) between 0.9 and 0.99) and amount as well as type of eutectic [29]. Similarly, the effect of Zn content on HTS of Mg–2Ca–xZn alloys is discussed and compared with that of Mg–0.5Ca–xZn alloys.

It is well established that a large freezing range (FR) leads to a high HTS [3]. Moreover, HTS is extremely sensitive to the susceptible temperature range (ΔT_s)[29, 33, 34]. The FR and ΔDT_s of Mg–2Ca–xZn alloys are listed in Table 2. In general, adding Zn to Mg–2Ca alloys widens the FR of Mg–2Ca–xZn alloys.

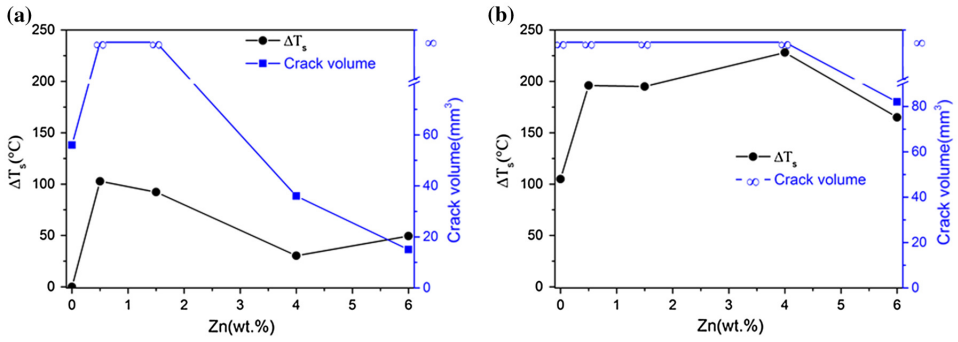

Figure 15: Comparison between ΔT_s and crack volumes (cast at T_{mould} = 250 °C) of a Mg–2Ca–xZn, b Mg–0.5Ca–xZn alloys

The FR significantly increases with 0.5 wt% Zn then decreases marginally with increasing Zn content until 4 wt% Zn (Mg–2Ca–4Zn). Then, further increase in the Zn content increases the FR (Mg–2Ca–6Zn). The ΔTs of the alloys also follows the similar trend.

Quantified crack volumes (Fig. 10) are used to evaluate the HTS of Mg–2Ca–xZn alloys: large crack volumes indicate a high HTS. In addition, a good correlation between ΔT_s and HTS is also found: a large ΔT_s results in a high HTS. In Eskin et al.'s study [35], high contraction during solidification is found in alloy with large susceptible solidification range (large ΔT_s). Such high contraction finally results in high HTS. Thus, alloy with a large ΔT_s normally has a high HTS. The tear volumes (represent the HTS) of alloys (cast at T_{mould} = 250 °C) and ΔT_s for the alloys are plotted against Zn content in Fig. 15a. As expected, both the curves follow a similar trend, however, they differ at 6 wt% Zn content. Despite the slightly higher ΔT_s compared to that of the Mg–2Ca–4Zn alloy, the Mg–2Ca–6Zn alloy has a lower crack volume. This discrepancy indicates that hot tearing is a complex phenomenon and ΔT_s is not the only underlying factor in?uencing hot tear formation.

The crack volume and ΔT_s for Mg–0.5Ca–xZn alloys as a function of Zn content are shown in Fig. 15b. It also reveals that a large ΔT_s results in a high HTS in Mg– 0.5Ca–xZn alloys. It should be noted that Mg–2Ca–xZn alloys have a lower ΔT_s than that of Mg–0.5Ca–xZn alloys with a fixed Zn content. Similarly, Mg–0.5Ca–xZn alloys have a higher HTS (larger crack volume) than that of Mg–2Ca–xZn alloys. For instance, Mg–0.5Ca, Mg–0.5Ca– 0.5Zn, Mg–0.5Ca–1.5Zn and Mg–0.5Ca–4Zn alloys were completely broken (cast at T_{mould} = 250 °C), while for Mg–2Ca–xZn alloys, only Mg–2Ca–0.5Zn and Mg–2Ca–1.5Zn alloys were completely broken. Besides, at a high mould temperature of 450 °C, no visible tears were observed in Mg–2Ca–xZn alloys, while in the case of Mg–

0.5Ca–xZn alloys, Mg–0.5Ca–1.5Zn and Mg–0.5Ca–4Zn alloys were still completely broken [29]. Although ΔT_s is not the only factor in?uencing the HTS, such results prove again that ΔT_s plays an important role on the HTS.

Amount of eutectic also plays an important role in in?uencing the hot tearing of Mg–2Ca–xZn alloys. In Suyitno et al.'s study, it is concluded that in direct chill casting of Al–Cu alloys, the amount of nonequilibrium eutectics can serve as a structure indicator of susceptibility to hot tearing [36]. The Al–Cu alloys with higher amount of nonequilibrium eutectics exhibit a lower HTS. Thus, the effect of nonequilibrium eutectics on HTS of Mg–2Ca–xZn alloys is discussed.

Large amount of devoiced eutectic segregation is mainly found in alloys cast at T_{mould} = 250 °C and rare at T_{mould} = 450 °C. The following discussion is based on the liquid healing of cracks in alloys cast at T_{mould} = 250 °C. In fact, eutectic structure is mainly observed near the tears instead of the exact sprue-rod junction (Fig. 9). Its existence at these specific locations indicates that the formation of eutectic and tear is somehow related. After the hot tears occur, the regions near them have a negative pressure. This negative pressure can suck back the residual liquid, and the cracks can be refilled [9]. Due to the nonequilibrium solidification, the residual liquid (at the time of hot tearing formation) enriches in solute. Such solute-enriched liquid continues transformation to the solid until the temperature reaches the eutectic temperature. At last, the eutectic is formed from the last remaining liquid at eutectic temperature and appears as eutectic segregation on the SEM micrograph [37]. Many previous investigations have shown that the eutectic liquid can completely or partially heal the previously formed hot cracks in binary Al–Cu [37, 38], Mg–Al, Mg–Zn and Mg–Y alloys [9, 39]. In direct chill casting of Al–Cu binary alloys, a thick line of eutectic (or eutectic path) along grain boundaries of several grains is observed near the tear region [37, 38]. Such eutectic is interpreted as a healed crack that has been filled with the liquid during the last stages of solidification [37]. Wang et al. [9] and Srinivasan et al. [10] have observed the presence of eutectic near the crack regions in Mg–Y and Mg–Gd alloys, respectively, and suggested that the cracks can be healed partially or completely by eutectic liquid during solidification.

The isopleths along Zn axis through Mg–Ca–Zn ternary phase diagram at a constant 2 wt% Ca are shown in Fig. 16. The isopleth is calculated using Pandat software and Scheil solidification model. According to the isopleth, three eutectic reactions may occur in Mg–2Ca–(0–6) Zn alloys:

(i) $L \rightarrow \alpha$-Mg + Mg_2Ca, 517 °C,

(ii) $L \rightarrow \alpha$-Mg + Mg_2Ca + $Mg_6Ca_2Zn_3$, 394 °C and

(iii) $L \rightarrow \alpha$-Mg + $Mg_6Ca_2Zn_3$ + MgZn, 295 °C.

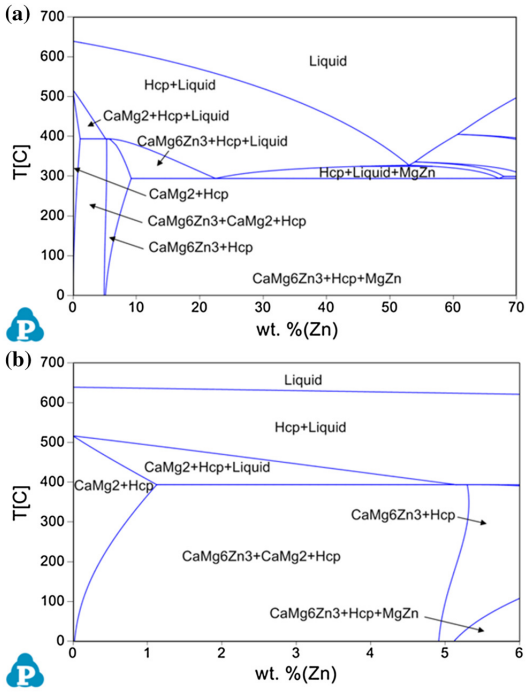

Figure 16: Isopleths along Zn axis through Mg–Ca–Zn ternary phase diagram at a constant 2 wt% Ca with a Zn content of a 0–70 wt%, b 0–6 wt%. The isopleth is calculated by Pandat with the PanMg_2014 database

	Mg-2Ca	Mg-2Ca-0.5Ca	Mg-2Ca-1.5Zn	Mg-2Ca-4Zn	Mg2Ca-6Zn
f_{lnes}	0.110	0.009	0.029	0.079	0.007
f_{el}	0.110	0.009	0.029	0.079	0.111

Table 3: Calculated liquid fractions at the nonequilibrium solidus (f_{lnes}) and eutectic liquid (f_{le}) in Mg–2Ca–xZn alloys

Generally, in binary alloy systems, the eutectic liquid (fle, mole fraction) is defined as the liquid fraction at the final eutectic temperature (end of solidification, nonequilibrium solidus). Thus, the eutectic liquid of Mg–2Ca alloy is taken as the liquid fraction at the nonequilibrium solidus of 517 °C, as listed in Table 3. However, in ternary Mg–Ca–Zn alloy systems, due to the complex eutectic reactions, it may not be appropriate to take the liquid fraction at the nonequilibrium solidus as the eutectic liquid. For instance, the liquid fractions at nonequilibrium solidus (f_lnes) of Mg–2Ca–xZn alloys calculated using Pandat thermodynamic software and Scheil solidification model are listed in Table 3. The f_lnes for Mg–2Ca–6Zn alloy is found to be relatively low.

However, both X-ray tomography studies (Fig. 9) and SEM analysis (Fig. 13) confirm that Mg–2Ca–6Zn contains maximum eutectic among all the alloys. Thus, it is proposed that the liquid fraction at the temperature of the eutectic reaction ii (394 °C) is the proper "eutectic liquid" for Mg–2Ca–6Zn alloy. The fle for Mg–2Ca–6Zn is 0.111, which is the largest among all (Table 3). The fle value for Mg–2Ca–xZn alloys increases with increase in Zn content, which agrees well with SEM analysis (Fig. 13). The proposal is further supported by the following experimental observations: Firstly, the crack initiation of Mg–2Ca–6Zn occurs before the eutectic reaction ii during solidification.

According to the force curves (Fig. 6), crack is initiated at 505 °C, whereas the eutectic reaction ii occurs at 394 °C for Mg–2Ca–6Zn alloy. Thus, the eutectic liquid of α-Mg + Mg_2Ca + $Mg_6Ca_2Zn_3$ eutectic refills the cracks and thus heals the cracks. Secondly, the SEM results confirm that the eutectic structure of Mg–2Ca–6Zn alloy mainly consists of Mg6Ca2Zn3 phase and a-Mg. The absence of Mg_2Ca and MgZn in the eutectic structure is likely due to their small amount. As Mg–2Ca–6Zn alloy has the maximum eutectic among all, it is expected to exhibit the best crack healing ability among all. As a result, although ΔT_s of Mg–2Ca– 6Zn alloy is slightly larger than that of Mg–2Ca–4Zn alloy, the final crack volume (HTS) of Mg–2Ca–6Zn is less than that of Mg–2Ca–4Zn alloy.

The higher HTS in Mg–0.5Ca–xZn alloys than that in Mg–2Ca–xZn alloys also lies in their different liquid healing behaviours. Small amount of eutectic and large amount of torn liquid film agglomerates on the fracture surface were

observed in high-Zn-containing Mg–0.5Ca– xZn alloys, such as Mg–0.5Ca–4Zn and Mg–0.5Ca–6Zn alloys [29]. On the contrary, in the case of Mg–2Ca–4Zn and Mg–2Ca–6Zn alloys, large amount of eutectic (Fig. 13d, e) and small amount of torn liquid film agglomerates (Fig. 14d) were observed. Such observations indicate that the remaining liquid at the time of hot tearing tends to form bulk eutectic in Mg–2Ca–xZn alloys and torn liquid films in Mg–0.5Ca–xZn alloys. As only the large bulk eutectic was able to heal the previously formed hot tears, it is concluded that Mg–2Ca–xZn alloys have a better cracking healing ability than Mg–0.5Ca–xZn alloys. Consequently, Mg–2Ca–xZn alloys have a better hot tearing resistance than Mg–0.5Ca–xZn alloys.

4.2 Influence of mould temperatures

HTS dramatically decreases with increase in the mould temperature for all the investigated alloys. Generally, high mould temperature improves the hot tearing resistance due to a reduction in thermal gradient and better compensation of strain [40]. During solidification, thermal gradients within the melt may result in regions of localised strain. Hot tearing occurs only if such accumulated thermal strain exceeds a critical value of strain in the casting [4, 41]. Normally, a lower cooling rate results in a smaller thermal gradient. With a lower cooling rate (high initial mould temperature), the solidification is closer to an equilibrium state, which results in lower contraction strain. Such low contraction strain leads to low HTS.

The cooling curves at hot spots of Mg–2Ca–xZn alloys are displayed in Figs. 6 and 7. As mentioned earlier, the cooling rates of alloys are around 0.56 and 0.22 °C/s at T_{mould} = 250 and 450 °C, respectively. Thus, the significantly decreased cooling rate leads to the highly improved hot tearing resistance at T_{mould} = 450 °C.

As solidification of a casting at a high initial mould temperature takes a longer time, the accumulated contraction strain can be better accommodated through microscopic movements of the dendrite cells or liquid metal [34]. The long solidification time provides adequate time to compensate for the accumulated strain. However, the time for compensation may not be sufficient during a faster solidification process (low initial mould temperature). In addition, due to the slower cooling at a high initial mould temperature, the solutes distributed uniformly. This is evidenced in the microstructures of Mg–2Ca–xZn alloys cast at both mould temperatures (Figs. 2, 5), as solute segregation was only observed in alloys cast at Tmould = 250 °C. Such solute segregation is likely to result in high HTS, as strain may concentrate on the solute segregated region. In other words, no such solute segregation is observed in alloys cast at high initial mould temperature and hence, hot tearing severity decreases.

5 Summary

Effect of Zn additions on hot tearing behaviour of Mg– 2Ca–xZn alloys were investigated. The cracking mechanism is also discussed. The following conclusions are drawn:

1. Adding Zn to Mg–2Ca–xZn alloys increases the hot tearing susceptibility (HTS) with a Zn content up to 1.5 wt%, and decreases with further Zn addition to 4 and 6 wt%.

2. High initial mould temperature dramatically decreases the HTS of Mg–2Ca–xZn alloys as a small thermal gradient and better accommodation of strain are expected at a higher mould temperature.

3. In the present study, as the actual tear location of alloys cast at low mould temperature is slightly shifted from the expected sprue-rod junction, where the temperature measurement was carried out, the solid fractions corresponding to the tearing initiation (f_{si}) for Mg–2Ca–xZn alloys are found low.

4. The hot tears initiate at grain boundaries and propagate along the grain boundaries through the thin film rupture and liquid metal embrittlement of solid bridges.

5. A good correlation between susceptible temperature range (ΔT_s) and HTS is observed for Mg–2Ca–xZn alloy. Generally, high ΔT_s results in a high HTS. ΔT_s of Mg–2Ca–xZn alloys increases with Zn addition, reaches a maximum of 103 °C with 0.5Zn (Mg–2Ca– 0.5Zn), and then decreases at higher Zn content.

6. The healing of hot tears by eutectic is evident in Mg– 2Ca–xZn alloys, especially at a mould temperature of 250 °C. Eutectic healing does not always occur at the final eutectic temperature for ternary alloys due to insufficient amount of liquid. It also happens before the final eutectic temperature. Large amount of eutectic is observed near the tear of Mg–2Ca and Mg–2Ca–6Zn alloys, indicating that these two alloys have a good cracking healing ability.

Acknowledgments

The authors would like to thank Mrs. Petra Fischer, Mr. Günter Meister, Mr. Gert Wiese for their technical supports. Financial support from China Scholarship Council for this work is greatly appreciated.

References

1. D'Elia F, Ravindran C, Sediako D (2015) Interplay among solidification, microstructure, residual strain and hot tearing in B206 aluminum alloy. Mater Sci Eng A 624:169–180

2. Easton MA, Gibson MA, Zhu SM, Abbott TB (2014) An a priori hot-tearing indicator applied to die-cast magnesium-rare earth alloys. Metall Mater Trans A 45:3586–3595

3. Cao G, Zhang C, Cao H, Chang YA, Kou S (2010) Hot-tearing susceptibility of ternary mg-al-sr alloy castings. Metall Mater Trans A 41:706–716

4. Eskin DG, Suyitno Katgerman L (2004) Mechanical properties in the semi-solid state and hot tearing of aluminium alloys. Prog Mater Sci 49:629–711

5. Sweet L, Easton MA, Taylor JA et al (2013) Hot tear susceptibility of Al-Mg-Si-Fe alloys with varying iron contents. Metall Mater Trans A 44:5396–5407

6. Cao G, Kou S (2006) Hot cracking of binary Mg–Al alloy castings. Mater Sci Eng A 417:230–238

7. Zhen Z, Hort N, Huang YD, Petri N, Utke O, Kainer KU (2009) Quantitative determination on hot tearing in Mg-Al binary alloys. Mater Sci Forum 618–619:533–540

8. Zhou L, Huang YD, Mao PL, Kainer KU, Liu Z, Hort N (2011) Influence of composition on hot tearing in binary Mg–Zn alloys. Int J Cast Met Res 24:170–176

9. Wang Z, Huang YD, Srinivasan A, Liu Z, Beckmann F, Kainer KU, Hort N (2013) Hot tearing susceptibility of binary Mg–Y alloy castings. Mater Design 47:90–100

10. Srinivasan A, Wang Z, Huang Y, Beckmann F, Kainer K, Hort N (2013) Hot tearing characteristics of binary Mg-Gd alloy castings. Metall Mater Trans A 44:2285–2298

11. Gunde P, Schiffl A, Uggowitzer PJ (2010) Influence of yttrium additions on the hot tearing susceptibility of magnesium–zinc alloys. Mater Sci Eng A 527:7074–7079

12. Wang Z, Song J, Huang YD, Srinivasan A, Liu Z, Kainer K, Hort N (2015) An investigation on hot tearing of Mg-4.5Zn-(0.5Zr) alloys with Y additions. Metall Mater Trans A 46:2108–2118

13. Cao G, Kou S (2006) Hot tearing of ternary Mg-Al-Ca alloy castings. Metall Mater Trans A 37:3647–3663

14. Cao G, Haygood I, Kou S (2010) Onset of hot tearing in ternary Mg-Al-Sr alloy castings. Metall Mater Trans A 41:2139–2150

15. Zhou L, Huang YD, Mao PL, Kainer KU, Liu Z, Hort N (2011) Investigations on hot tearing of Mg-Zn-(Al) alloys. In: Sillekens WH, Agnew SR, Neelameggham NR, Mathaudhu SN (eds) Magnesium technology. Wiley, Hoboken, pp 125–130

16. Wang Y, Wang Q, Wu G, Zhu Y, Ding W (2002) Hot-tearing susceptibility of Mg–9Al–xZn alloy. Mater Lett 57:929–934

17. Bakhsheshi-Rad HR, Idris MH, Abdul-Kadir MR (2013) Synthesis and in vitro degradation evaluation of the nano-HA/MgF_2 and DCPD/MgF_2 composite coating on biodegradable Mg–Ca– Zn alloy. Surf Coat Tech 222:79–89

18. Zhang B, Hou Y, Wang X, Wang Y, Geng L (2011) Mechanical properties, degradation performance and cytotoxicity of Mg–Zn– Ca biomedical alloys with different compositions. Mater Sci Eng C 31:1667–1673

19. Zhang B, Wang Y, Geng L (2011) Mechanical properties, degradation performance and cytotoxicity of Mg–Zn–Ca biomedical alloys with different compositions. In: Pignatello R (ed) Biomaterials—physics and chemistry. InTech, Rijeka, pp 183–204

20. Gao X, Zhu SM, Muddle BC, Nie JF (2005) Precipitation-hardened Mg–Ca–Zn alloys with superior creep resistance. Scripta Mater 53:1321–1326

21. Tong LB, Zheng MY, Hu XS, Wu K, Xu SW, Kamado S, Kojima Y (2010) Influence of ECAP routes on microstructure and mechanical properties of Mg–Zn–Ca alloy. Mater Sci Eng A 527:4250–4256

22. Somekawa H, Mukai T (2007) High strength and fracture toughness balance on the extruded Mg–Ca–Zn alloy. Mater Sci Eng A 459:366–370

23. Levi G, Avraham S, Zilberov A, Bamberger M (2006) Solidification, solution treatment and age hardening of a Mg–1.6 wt% Ca–3.2 wt% Zn alloy. Acta Mater 54:523–530

24. Nie JF, Muddle BC (1997) Precipitation hardening of Mg-Ca(-Zn) alloys. Scripta Mater 37:1475–1481

25. Tong LB, Zheng MY, Xu SW et al (2011) Effect of Mn addition on microstructure, texture and mechanical properties of Mg–Zn– Ca alloy. Mater Sci Eng A 528:3741–3747

26. Gao JH, Guan SK, Ren ZW, Sun YF, Zhu SJ, Wang B (2011) Homogeneous corrosion of high pressure torsion treated Mg–Zn– Ca alloy in simulated body fluid. Mater Lett 65:691–693

27. Song J, Wang Z, Huang YD, Srinivasan A, Beckmann F, Kainer KU, Hort N (2015) Hot tearing susceptibility of Mg-Ca binary alloys. Metall Mater Trans A 46:6003–6012

28. Powell BR, Luo AA, Tiwari BL, Rezhets V (2002) The die castability of calcium-containing magnesium alloys: thin-wall computer case, Magnesium Technology 2002. TMS, Warrendale, pp 123–129

29. Song J, Wang Z, Huang YD, Srinivasan A, Beckmann F, Kainer KU, Hort N (2015) Effect of Zn addition on hot tearing behaviour of Mg–0.5Ca–xZn alloys. Mater Design 87:157–170

30. Zhen Z, Hort N, Utke O, Huang YD, Petri N, Kainer KU (2009) Investigations on hot tearing of Mg-Al binary alloys by using a new quantitative method. In: Nyberg EA, Agnew SR, Neelameggham NR, Pekguleryuz MO (eds) Magnesium Technology. Wiley, Hoboken, pp 105–110

31. D'Elia F, Ravindran C, Sediako D, Kainer KU, Hort N (2014) Hot tearing mechanisms of B206 aluminum–copper alloy. Mater Design 64:44–55

32. Eskin DG, Katgerman L (2007) A quest for a new hot tearing criterion. Metall Mater Trans A 38:1511–1519

33. Clyne TW, Davies GJ (1979) Comparison between experimental data and theoretical predictions relating to dependence of solidification cracking on composition. Solidification and casting of metals. Metals Society, London, pp 275–278

34. Wang Z, Huang Y, Srinivasan A, Liu Z, Beckmann F, Kainer K, Hort N (2014) Experimental and numerical analysis of hot tearing susceptibility for Mg–Y alloys. J Mater Sci 49:353–362. doi:10. 1007/s10853-013-7712-z

35. Eskin DG, Suyitno Mooney JF, Katgerman L (2004) Contraction of aluminum alloys during and after solidification. Metall Mater Trans A 35:1325–1335

36. Suyitno Eskin DG, Savran VI, Katgerman L (2004) Effects of alloy composition and casting speed on structure formation and hot tearing during direct-chill casting of Al-Cu alloys. Metall Mater Trans A 35:3551–3561

37. Eskin DG, Savran VI, Katgerman L (2005) Effects of melt temperature and casting speed on the structure and defect formation during direct-chill casting of an Al-Cu alloy. Metall Matrt Trans A 36:1965–1976

38. Suyitno Eskin DG, Katgerman L (2006) Structure observations related to hot tearing of Al-Cu billets produced by direct-chill casting. Mater Sci Eng A 420:1–7

39. Huang YD, Wang Z, Srinivasan A, Kainer KU, Hort N (2012) Metallurgical characterization of hot tearing curves recorded during solidification of magnesium alloys. Acta Phys Pol A 122:497–500

40. Huang H, Fu P, Wang Y, Peng L, Jiang H (2014) Effect of pouring and mold temperatures on hot tearing susceptibility of AZ91D and Mg–3Nd–0.2Zn–Zr Mg alloys. Trans Nonferr Met Soc 24:922–929

41. Pellini WS (1952) Strain theory of hot tearing. Foundry 80:125–199